JOURNAL OF MATERIALS SCIENCE **38** (2003) 1559– 1564

The fragmentation of primary dendrites during shearing in semisolid processing

S. JI
Brunel Centre for Advanced Solidification Technology (BCAST), Brunel University, Uxbridge, Middlesex, UB8 3PH, UK
E-mail: mtsrssj@brunel.ac.uk

Semisolid slurries with non-dendritic microstructure can be produced by solidification under forced convection. Dendrite fragmentation is a commonly accepted mechanism for shearing semisolid slurry. However, it requires from experimental observation to confirm the fragmentation of dendrite arms occurring during shearing process. Experiments are undertaken to investigate the dendrite fragmentation in Sn-15wt%Pb alloy under shearing by virtue of a twin-screw extruder together with the wetting and penetration of pure tin grain boundaries submerged and sheared in the semisolid slurry of Sn-15wt%Pb alloy. It is found that the primary dendrites can be fragmented rapidly into small particles and there are penetration grooves existing in the partially fragmented dendrites. Such grooves are similar to that found at the grain boundaries in pre-cast pure tin polycrystals, which have been submerged and sheared in the semisolid slurry of Sn-15wt%Pb alloy.

1. Introduction

Semisolid metal (SSM) processing is based on the unique non-dendritic microstructures, which can be produced by applying shear deformation when a liquid alloy is cooled through the temperature interval between its liquidus and solidus [1, 2]. Instead of the conventional dendrites, the microstructure of sheared semisolid slurry is characterised by rosettes and/or spheroidal primary particles dispersed in liquid matrix [3]. Over the last few decades, there have been many mechanisms proposed to describe the formation of the non-dendritic microstructures during semisolid processing, which include cellular growth [4, 5], dendrite fragmentation [6], recalescence [7, 8], spheroidal growth [9]. Of these hypotheses, dendrite fragmentation is the most popular mechanism.

Flemings [10] has listed a number of possible mechanisms for fragmentation of dendrite arms, which may be summarised as three main groups: (1) dendrite arms break off at their roots due to shear forces; (2) dendrite arms melt off at their roots; and (3) dendrite arms bend under flow stresses creating boundaries within the bent dendrites followed by complete wetting of high angle, high energy grain boundaries by liquid phase leading to eventual break-up of dendrites. The third group was known as grain boundary wetting mechanism, which was proposed by Vogel [6] and further discussed by Doherty and Cantor *et al*. [11, 12]. In the earlier studies, both low angle and low energy boundaries and high angle and high energy were found in sheared microstructures and recognised as the result of grain boundary wetting and penetration [13, 14], the recent study carried by Xia *et al.* has confirmed that the low angle and low energy boundaries between different particles are actually from a single primary crystal with a fairly complicated structure forming pseudo-particles in an across section [15]. They also confirmed that the misorientation from different particles belonging to different crystals are usually greater than 10°. There were also a few publications supporting grain boundary wetting/penetration mechanism. A series studies carried by Lee *et al.* [14, 16, 17] have shown the observation of dislocation pileups at subgrain boundaries in a sheared Al-Si alloy. Cheng *et al.* found the distinction between non-solute-enriched boundaries formed by recrystallization and the solute-enriched boundaries formed by surfaces sintering of solute-enriched particles [18]. Theoretical simulation carried out by Mullins also indicated that the dendrite arms can be bent in thermal/solutal advection during fluid flow in semisolid temperature [19]. However, there is still limited information about the dendrite fragmentation during shearing of a partially solidified alloy, in particular, the fragmentation procedure under high shear rate. There is no direct observation of partially wetted grooves in the bent dendritic arms.

The present work aims to study the dendrite fragmentation procedure of the partially solidified Sn-15wt%Pb alloy under high shear rate and to observe the wetted grooves in bent dendrite arms. Therefore, a recently developed twin-screw extruder which can offer high shear rate and high intensity of turbulence during SSM processing was used to directly shear the partially solidified Sn-15wt%Pb alloy. The wetting procedure along grain boundaries was observed using a simulated method by submerging and shearing pure Sn polyscrystals in Sn-15wt%Pb liquid-solid mixture. Discussions are

made on the mechanism of dendrite fragmentation of Sn-15wt%Pb semisolid slurry.

2. Experimental

2.1. Isothermal shearing of solid-liquid mixture with dendritic structure

The dendrite fragmentation experiments were carried out using a laboratory scale twin-screw extruder (Fig. 1), which is the core of the newly developed twin-screw rheomoulding equipment. A detailed description of the twin-screw rheomoulding process and equipment can be found in Ref. [20]. The twin-screw extruder consists of a pair of closely intermeshing, self-wiping and co-rotating screws positioned in a barrel with an accurate temperature control and an outlet valve. The fluid flow in the extruder is characterised by high shear rate, high intensity of turbulence and cyclic variation of shear rate. The shear rate used in this work refers to that between the inner surface of the barrel and the tip of the screw flight and is defined as:

$$\dot{\gamma} = \pi N(D/\delta - 2) \tag{1}$$

where D is the interal diameter of the barrel, δ is the gap between the inner surface of the barrel and the tip of the screw flight, and N is the rotation speed. The twin-screw extruder can be operated either at a predetermined temperature for isothermal shearing or at a predetermined shear rate during continuous cooling with a controlled cooling rate. The melt temperature was directly measured by a thermocouple immersed into the melt at the end of the extruder.

A Sn-15wt%Pb alloy was prepared by melting the industrially pure tin and lead with a purity >99.8%. The melted Sn-15wt%Pb alloy in a graphite crucible with about 50°C overheat was cooled down to 220°C and subsequently fed into the twin-screw extruder with right quantity. The fed melt was isothermally maintained at 215°C for 5 min and then cooled down to 206°C at 0.5°C/min. Once the melt reached 206°C, the extruder started to run at a pre-set rotation speed, which resulted in the isothermal shearing of solid-liquid mixture with dendritic structure. The sheared semisolid slurry was directly discharged into cold water after different shearing times for subsequent microstructure examination.

The samples were ground and polished using a standard metallographycal procedure down to 1 μm. The microstructures of the samples were characterised using optical microscope (OM) and JEOL-840 scanning electron microscope (SEM). The shape factor, F, is defined here as:

$$F = 4\pi A/P^2 \tag{2}$$

where A and P are the projecting area and the peripheral length of the primary particles. The size and the volume fraction of the primary particles under various processing conditions were measured with an image analyser, in which at least 500 particles were examined. For samples without shearing, the whole dendrite was regarded as one grain and the outline was used to define the grain size and perimeter.

2.2. Grain boundary penetration

In order to confirm the groove formation along the grain boundaries during shearing semisolid slurry, a simulation experiment was designed by shearing a pre-cast Sn crystals in the solid-liquid mixture of Sn-15wt%Pb alloy. The grain boundary penetration experiments were carried out in a device schematically shown in Fig. 2, which consisted of a furnace, a motor, a sample holder and a positioning device. The semisolid slurry was hold in a Φ60 mm crucible with 100 mm in depth. The rotation speed of the sample was detected by a transducer and controlled within ±5 rpm.

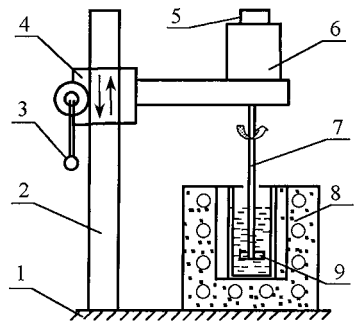

1-mounting base; 2-piller; 3-handler; 4-gear box; 5-speed detector; 6-motor; 7-stirrer; 8-furnace; 9-sample

Figure 2 Schematic illustration of the stirring device used in the current experiments.

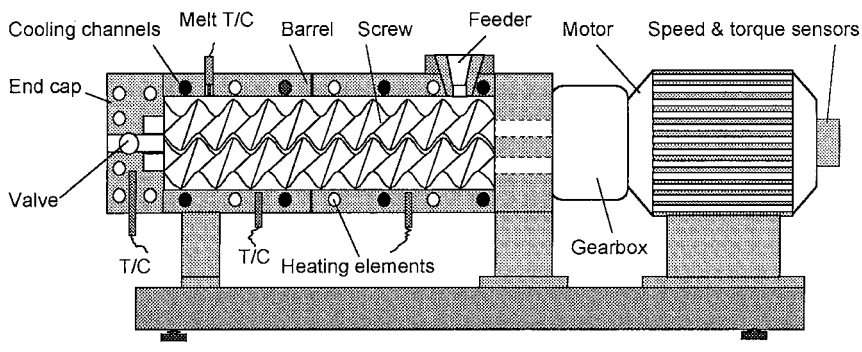

Figure 1 The schematic illustration of a laboratory scale twin-screw extruder used for current experiments.

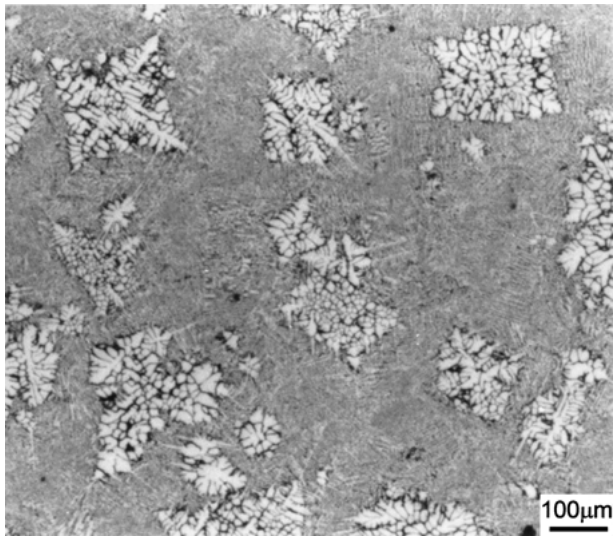

Figure 3 Micrographs showing the microstructure of Sn-15wt%Pb alloy cooled naturally from 220°C to 206°C and water-quenched from 206°C.

The pure tin sample was produced by melting industrial pure tin (>99.8%) and cast into a steel mould with an external dimension of $\Phi 100 \times 170$ mm and a preheated temperature of 200°C. The melt was poured into the mould with about 30°C overheat and solidified naturally to form an ingot with in a dimension of $\Phi 32 \times 130$ mm. The ingot was cut, ground and polished to form a sample of $10 \times 10 \times 35$ mm. The sample was then fastened at one end of the stirrer. Meanwhile, the industrially pure tin and lead were melted in a furnace to form Sn-15wt%Pb melt with about 50°C overheat, and then the temperature of the melt was stabilised to the semisolid processing temperature of 202°C while the stirring was applied. At 202°C, the pure tin sample was submerged into the semisolid slurry and rotated with 300 rpm for different times before taken out for microstructure examination. The microstructures of the samples were characterised using a JEOL-840 scanning electron microscope.

3. Results

3.1. Dendrite fragmentation

Fig. 3 shows the microstructure of Sn-15wt%Pb alloy water-quenched from 206°C without shearing, demonstrating a coarse dendrite structure of the primary phase in the matrix. The dendrites are equiax with entrapped liquid. Fig. 4 shows the fragmentation behaviour of dendrites in the solid and liquid mixture of Sn-15wt%Pb alloy sheared isothermally at 206°C with a shear rate of 2041 s^{-1} for different shearing times. The results indicated that the volume fraction of the primary phase was consistent at 20% for different isothermal shearing times. At the beginning of the isothermal shearing, the original dendrites were quickly fragmented into small segments (Fig. 4a). With increasing isothermal shearing time, the dendrites were further broken down to smaller particles (Fig. 4b) and eventually spheroidised (Fig. 4c). After this, the further shearing did not significantly affect the spheroidal morphology of Sn-15wt%Pb alloy (Fig. 4d). The measured average intercept lengths of the

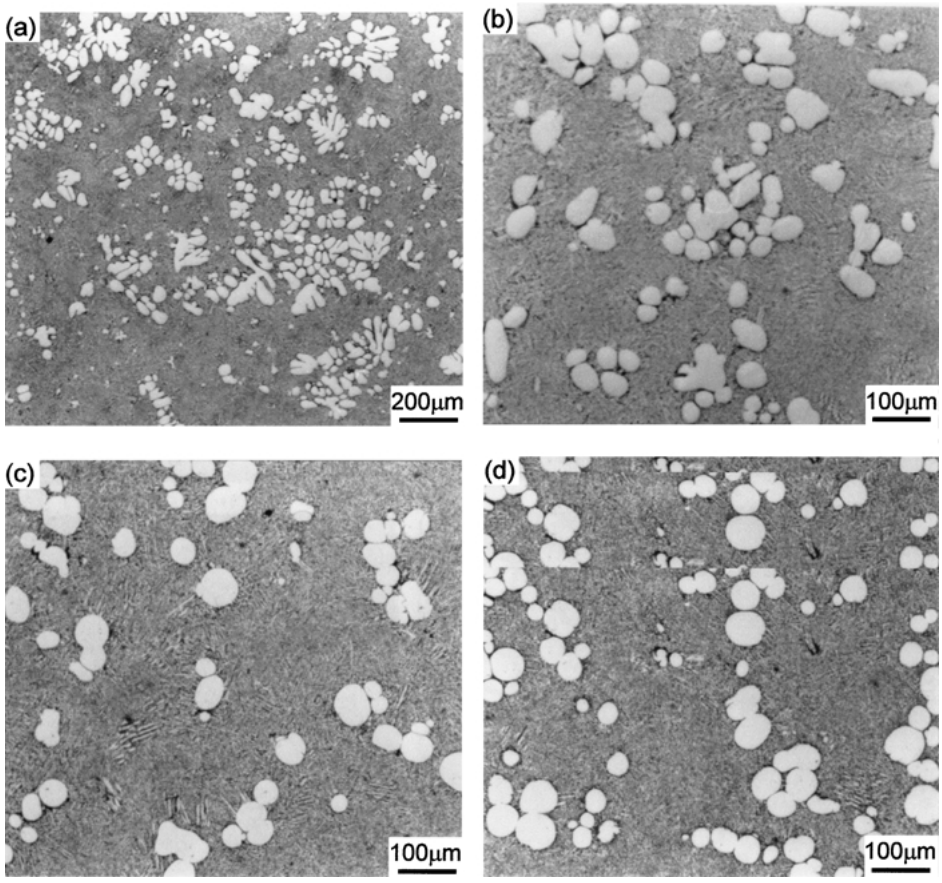

Figure 4 Micrographs showing the microstructure of Sn-15wt%Pb alloy after isothermal shearing the initially formed dendrites at 206°C with a shear rate of 2041 s^{-1} for different times. (a) 2 s, (b) 10 s, (c) 60 s, and (d) 750 s.

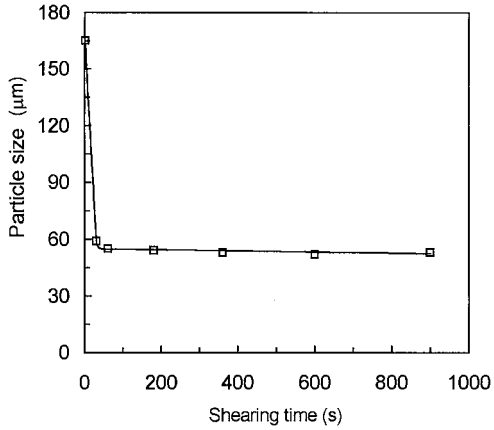

Figure 5 The average intercept length of the primary particles of Sn-15wt%Pb alloy sheared isothermally at 206°C with a shear rate of 2041 s^{-1} for dendritic fragmentation as a function of isothermal shearing time.

primary solid particles are shown in Fig. 5 as a function of isothermal shearing time. The initial dendrites and small dendritic segments were considered as particles including entrapped liquid. Clearly, the fragmentation of the dendrite occurred immediately after the shear was applied to the dendrite-containing solid-liquid mixture. The average particle size decreased very quickly with increasing the isothermal shearing time until it reached a stable value of 52 μm. The measured shape factors of primary particles are represented in Fig. 6 as a function of the isothermal shearing time. With increasing the isothermal shearing time, the shape factor of the primary particles increased to about 0.7 and then stayed around 0.7 with further shearing. The results in Figs 4–6 confirmed that the fragmentation was completed rapidly after applying shear and the spheroidisation took much longer time for Sn-15wt%Pb alloy. The sample in Fig. 4a was further examined with higher magnification in order to find out the existing wetted and/or penetrated grain boundaries in the fragmented dendrite arms. Fig. 7 shows the backscattered SEM micrographs, exhibiting clearly a typical groove on the bent Sn dendrites. The groove A in Fig. 7 was characterised by large angle, showing the state of liquid penetration. The groove B indicated a completely wetted grain boundary.

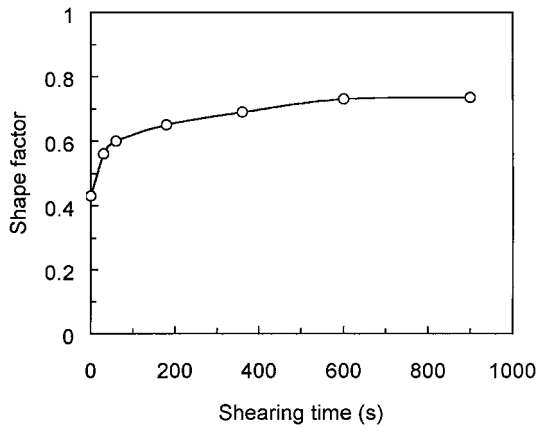

Figure 6 The effect of the shearing time on the shape factor of the primary particles in Sn-15wt%Pb alloy sheared isothermally at 206°C with a shear rate of 204 s^{-1}.

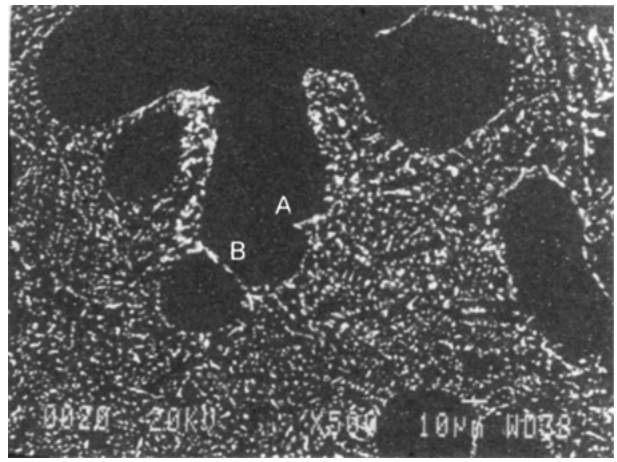

Figure 7 Backscattered SEM micrograph showing the penetration of liquid into the bent dendrite arms of partially solidified Sn-15wt%Pb alloy sheared isothermally at 206°C and 2041 s^{-1} for 2 s in the twin-screw extruder. A: a groove indicating the state of liquid penetration and B: complete penetration.

3.2. Grain boundary wetting

This experiment aimed to observe the wetting and penetration of the liquid in semisolid slurry along the grain

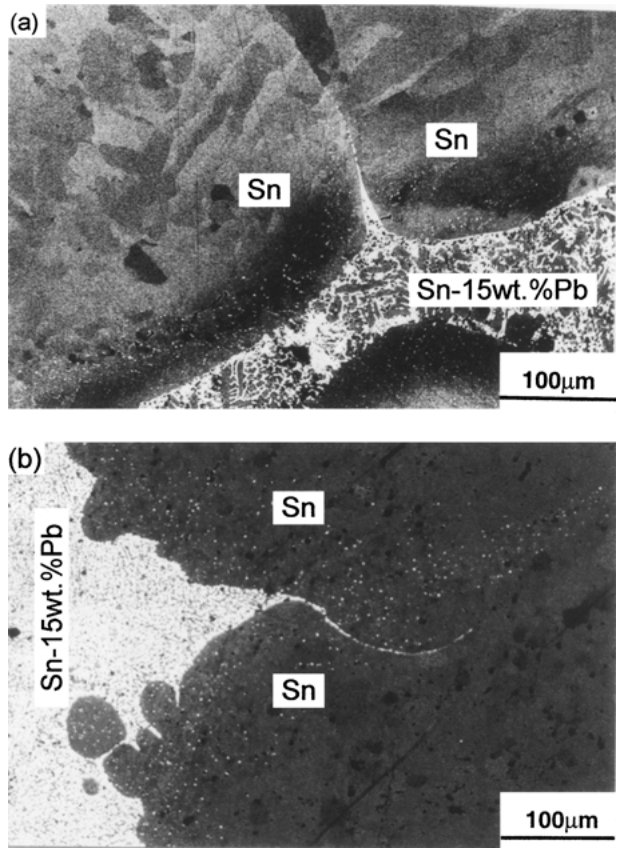

Figure 8 Backscattered SEM micrographs showing the Sn polycrystals exposed in Sn-15wt%Pb semisolid slurry and stirred isothermally at 202°C with 300 rpm for different times. (a) 60 min: large angle groove with short acute end penetrated along the Sn grain boundary and (b) 120 min: large angle groove with longer acute end penetrated along the Sn grain boundary.

boundaries in a pure Sn polycrystal. The liquidus and solidus temperature of Sn-15wt%Pb alloy are 210°C and 183°C respectively. So the penetration was set at 202°C, at which the volume fraction of the solid phase in Sn-15wt%Pb alloy was about 32%. Fig. 8 shows the backscattered SEM micrographs of groove profiles along grain boundary observed after submerging Sn polycrystals in the Sn-15wt%Pb semisolid slurry at 202°C for different times. Obviously, they were characterised by deep channels. The groove angles formed at the intersection of the grain boundary with the phase interface were very acute at the end of the tip and were large at the root of the groove closing to the semisolid slurry. Some small Pb particles were detected in the vicinity of the solid-liquid interface both along grain boundaries and on the sample surface. These small Pb particles were not uniform and all of them were smaller than 1 μm. The observations in this experiment are similar to those in the dendrite fragmentation experiments.

4. Discussion

4.1. Mechanism of dendrite fragmentation

The current experimental results indicate that shearing the initially formed dendrites in Sn-15wt%Pb alloy can cause dendrite fragmentation. The fragmentation occurs immediately after applying shear and completes within first few seconds and then undergoes a much slower particle spheroidisation process (Figs 4–6). The bent dendrite arms are penetrated by the liquid in semisolid slurry to form large angle grooves across the section (Fig. 7), resulting in the formation of fine and spherical primary particles. The experimental results also indicate that the grain boundaries in Sn polycrystals can be penetrated by the liquid in the semisolid slurry of Sn-15wt%Pb alloy. The results imply that the formation of the primary particles can be attributed to the penetration of the liquid along the grain boundaries in the bent dendrite arms formed during shearing semisolid slurry.

The grain boundaries are formed by recovery of the "geometrically necessary dislocations" generated by plastic bending of dendritic arms under viscous force [11, 12]. Liquid metal would subsequently wet the grain boundaries, resulting in the dendrite arm detachment. In this process, there are at least two stages: formation of grain boundaries in the dendrite arms and wetting along the grain boundaries.

The formation of the grain boundary in dendrite arms also includes a few stages, such as plastic bending deformation, dislocation migration and subgrain boundary formation. The plastic bending deformation is caused by shearing. Twin-screw rheomoulding is characterised by high shear rate and high intensity of turbulence [20], which would offer sufficient shearing force on semisolid slurry. There are four scaling groups, each consisting of different forces acting on the semisolid slurry in a twin-screw extruder. The first group relates to the scales of inertia forces and centrifugal forces; the second group concerns the scale of gravity force; the third comprises the scale of internal friction; and the fourth group refers to the scales of elastic and plastic deformation behaviour of the materials being processed. Therefore, the compression, rupture, shear and elasticity forces act on the semisolid slurry with a variation for every rotation. This means that the dendrite arms in the semisolid slurry experience vigorously forces during plastic deformation. Due to the low volume fraction of primary phase in the experiments and the size of the existing primary dendrites, it is difficult for mechanical force to directly break off the dendrite arms. The plastic deformation of the dendrite arms is more likely caused by vigorously viscous forces which further increases the dislocations and the stress concentration therein and eventually form microcracks in the bent dendrite arms. Even though it is very difficult to directly observe the dislocation migration and subgrain boundaries, the experimental observation (Fig. 7) reveals that the grooves could be formed during shearing in the dendrite arms of primary Sn phase. It should be noted that the breakdown might be very quick due to the high shear rate and high intensity of turbulence offered by twin-screw extruder, as shown in Fig. 4. The result in Fig. 8 with pre-cast pure Sn stirred in Sn-15wt%Pb semisolid slurry further confirms that the penetration of the liquid can only occur along the grain boundaries. Therefore, the observation of partially wetted groove in the dendrite arms during shearing semisolid slurry reveals that there is at least one grain boundary existing in the dendrite arms. Lee's observations [16, 17] with Al-Si alloy also confirm that the dislocation density is increased for the sheared dendrite arms and subgrain boundaries can form after the dislocation migration under shearing.

On the other hand, the formed grain boundaries should be wetted or penetrated by the liquid in the semisolid slurry. Even though Figs 7 and 8 have confirmed the existing of wetted grooves, the wetting and penetration procedure is actually very complex. The capillary equilibrium condition at the contact between the grain boundary and the liquid metal can be represented by: $\sigma_{GB} = 2\sigma_{SL}\cos(\theta/2)$, where σ_{GB} is the grain boundary free energy; σ_{SL} is the solid-liquid interface free energy; θ is the angle formed between the two σ_{SL} vectors. In the non-equilibrium wetting process, the energetic condition to form a wetted groove on the grain boundary is $\sigma_{GB} \geq 2\sigma_{SL}\cos(\theta/2)$. The difference $S = \sigma_{GB} - 2\sigma_{SL}\cos(\theta/2)$ can be understood as a wetting "driving force" leading to the formation of an intergranular groove [21]. A smaller groove angle θ can result in smaller wetting driving force. When the groove angle becomes equal to 0°, the grain boundaries are fully wetted, but the driving force reduces to a minimum value.

4.2. Applicability of the fragmentation mechanism

Attributing the formation of fragments to shearing is applicable for shearing partially solidified liquid-solid mixture. The shearing should have sufficient intensity and with turbulent flow to plastically bend the initial

dendrites and result in the formation of grain boundaries in the bent dendrite arms. The liquid in semisolid slurry could subsequently wet and penetrate the grain boundaries to form liquid films, which eventually break down the dendrites into small pieces. The wetting process is supposed to be rapid due to being close to liquidus temperature. If the shearing is insufficient of pure laminar flow, the dendrite arms are believed to form rosettes during bending and subsequently undergo rosette spheroidisation. So the eventual microstructure contains large spherical rosettes with entrapped liquid. If the shearing with high shear rate and high intensity of turbulence is applied to the liquid from a temperature above its liquidus to a temperature within the interval between liquidus and solidus, the vigorous turbulence flow would suppress the formation of dendrites at the early stage of solidification. The microstructural evolution in semisolid slurry will develop spheroidal growth [9, 20]. Therefore, the morphology of primary phase in semisolid slurry changes from spherical rosettes with entrapped liquid to spherical particles without entrapped liquid while increasing the shear rate and turbulence flow. The mechanism of dendrite arms remelt at their roots is just applicable for reheating process. If reheating a billet with a fine dendrite microstructure to a temperature within the interval between liquidus and solidus, the dendrites would be melted at roots. They undergo recalescence and Ostwald ripening mechanism due to lack of shearing and existing of temperature gradient.

5. Conclusions

Shearing partially solidified melt under high shear rate can result in the fragmentation of the initially formed dendritic structure and produce a fine spherical structure without entrapped liquid. The dendrite fragmentation in the partially solidified solid-liquid mixture occurs immediately after applying shearing and completes rapidly within first few seconds, but the spheroidisation of the fragmented particles under isothermal shearing is a relatively slow process. The dendrites are fragmented via the penetration of liquid into the bent dendrite arms to form large angle grooves along grain boundaries.

Acknowledgement

Appreciation goes to Professor Fan for his advice. The financial support from EPSRC and Ford Motor Co. are gratefully acknowledged.

References

1. D. B. SPENCER, R. MEHRABIAN and M. C. FLEMINGS, *Metall Trans.* A **3A** (1972), 1925.
2. P. A. JOLY, *J. Mater. Sci.* **11** (1976) 1393.
3. D. H. KIRKWOOD, *Inter. Mater. Rev.* **39** (1994) 173.
4. J. M. M. MOLENAAR, F. W. H. C. SALEMANS and L. KATGERMAN, *J. Mater. Sci.* **20** (1985) 4335.
5. J. M. M. MOLENAAR, L. KATGERMAN, W. H. KOOL and R. J. SMEULDERS, *ibid.* **21** (1986) 389.
6. A. VOGEL, *Metal Sci.* **12** (1978) 576.
7. A. HELLAWELL, in Proc. 4th Inter. Conf. on Semi-Solid Processing of Alloys and Composites, Sheffield, UK, June 1996, edited by D. H. Kirkwood and P. Kapranos (Great Britain, 1996) p. 60.
8. J. PILLING and A. HELLAWELL, *Metall. Trans.* A **27A** (1996) 229.
9. S. JI and Z. FAN, *ibid.* **33A** (2002), 3511.
10. M. C. FLEMINGS, *ibid.* **22A** (1991) 957.
11. A. VOGEL, R. D. DOHERTY and B. CANTOR, in Proc. Conf. on Solidification and Casting of Metals, Sheffield, UK, July 1977, edited by Metal Society (London, 1979) p. 518.
12. R. D. DOHERTY, H. LEE and E. A. FEEST, *Mater. Sci. Eng.* **65** (1984) 181.
13. N. APAYDIN, K. V. PRABHAKAR and R. D. DOHERTY, *ibid.* **46** (1980) 145.
14. H. I. LEE, R. D. DOHERTY, E. A. FEAST and J. M. TICHMARSH, in Proceedings of an Inter. Conf. at University of Warwick, Coventry, UK, 1980, edited by the Metals Society (London, 1980) p. 119.
15. B. NIROUMAN and K. XIA, *Mater. Sci. Eng.* A **A283** (2000) 70.
16. J. I. LEE, H. I. LEE and M. KIM, *Script. Mater.* **32** (1995) 1945.
17. J. I. LEE, H. I. KIM and H. I. LEE, *Mater. Sci. Tech.* **14** (1998) 770.
18. J. A. CHENG, D. APELLIAN and R. D. DOHERTY, *Metall. Trans.* A **17A** (1986) 2049.
19. A. M. MULLIS, *Acta Metall. Mater.* **47** (1999) 1783.
20. S. JI, Z. FAN and M. J. BEVIS, *Mater. Sci. Eng.* A **A299** (2001) 210.
21. P. J. DESRE, *Script Mater. Mater.* **37** (1997) 875.

Received 23 August 2001
and accepted 13 December 2002